Inorg. Chem. **2009**, *48*, 1407−1415

Possible Steric Control of the Relative Strength of Chelation Enhanced Fluorescence for Zinc(II) Compared to Cadmium(II): Metal Ion Complexing Properties of Tris(2-quinolylmethyl)amine, a Crystallographic, UV−Visible, and Fluorometric Study

Neil J. Williams,[†] Wei Gan,[†] Joseph H. Reibenspies,[‡] and Robert D. Hancock*[,†]

Department of Chemistry and Biochemistry, University of North Carolina at Wilmington, Wilmington, North Carolina 28403, and Department of Chemistry, Texas A&M University, College Station, Texas 77843

Received July 25, 2008

The idea is examined that steric crowding in ligands can lead to diminution of the chelation enhanced fluorescence (CHEF) effect in complexes of the small Zn(II) ion as compared to the larger Cd(II) ion. Steric crowding is less severe for the larger ion and for the smaller Zn(II) ion leads to Zn−N bond length distortion, which allows some quenching of fluorescence by the photoinduced electron transfer (PET) mechanism. Some metal ion complexing properties of the ligand tris(2-quinolylmethyl)amine (TQA) are presented in support of the idea that more sterically efficient ligands, which lead to less M−N bond length distortion with the small Zn(II) ion, will lead to a greater CHEF effect with Zn(II) than Cd(II). The structures of $[Zn(TQA)H_2O](ClO_4)_2 \cdot 1.5\ H_2O$ (**1**), $([Pb(TQA)(NO_3)_2] \cdot C_2H_5OH)$ (**2**), $([Ag(TQA)(ClO_4)])$ (**3**), and $(TQA) \cdot C_2H_5OH$ (**4**) are reported. In **1**, the Zn(II) is 5-coordinate, with four N-donors from the ligand and a water molecule making up the coordination sphere. The Zn−N bonds are all of normal length, showing that the level of steric crowding in **1** is not sufficient to cause significant Zn−N bond length distortion. This leads to the observation that, as expected, the CHEF effect in the Zn(II)/TQA complex is much stronger than that in the Cd(II)/TQA complex, in contrast to similar but more sterically crowded ligands, where the CHEF effect is stronger in the Cd(II) complex. The CHEF effect for TQA with the metal ions examined varies as Zn(II) ≫ Cd(II) ≫ Ni(II) > Pb(II) > Hg(II) > Cu(II). The structure of **2** shows an 8-coordinate Pb(II), with evidence of a stereochemically active lone pair, and normal Pb−N bond lengths. In **3**, the Ag(I) is 5-coordinate, with four N-donors from the TQA and an oxygen from the perchlorate. The Ag(I) shows no distortion toward linear 2-coordinate geometry, and the Ag−N bonds fall slightly into the upper range for Ag−N bonds in 5-coordinate complexes. The structure of **4** shows the TQA ligand to be involved in π-stacking between quinolyl groups from adjacent TQA molecules. Formation constants determined by UV−visible spectroscopy are reported in 0.1 M $NaClO_4$ at 25 °C for TQA with Zn(II), Cd(II), and Pb(II). When compared with other similar ligands, one sees that, as the level of steric crowding increases, the stability decreases most with the small Zn(II) ion and least with the large Pb(II) ion. This is in accordance with the idea that TQA has a moderate level of steric crowding and that steric crowding increases for TQA analogs tris(2-pyridylmethyl)amine (TPyA) < TQA < tris(6-methyl-2-pyridyl)amine (TMPyA).

Introduction

The development of fluorescent ligands for detection of Zn(II) by means of chelation enhanced fluorescence[1−18] (CHEF) is of interest, particularly as sensors for Zn(II) in nervous tissues.[1−18] Evidence suggests that Zn imbalances are involved in seizures that occur in epilepsy, neurodegenerative diseases, and traumatic brain damage,[11] and Zn(II) appears to play a role in the aggregation of β-amyloid peptide in the brain in Alzheimer's disease.[19] Synthesis of ligands that might be useful as selective sensors for the toxic Cd(II) ion is also of interest,[20−23] particularly in the environment in the presence of the ubiquitous Zn(II) ion. Most of these

* To whom correspondence should be addressed. E-mail: hancockr@uncw.edu.
[†] University of North Carolina at Wilmington.
[‡] Texas A&M University.

10.1021/ic801403s CCC: $40.75
Published on Web 01/14/2009

ligands for sensing Zn(II) or Cd(II) have pyridyl or quinolyl donor groups present, as primarily coordinating groups (pyridyls) or as fluorophores as well (quinolyls). The production of a CHEF effect depends on the photoinduced electron transfer (PET) mechanism. In the PET mechanism, electrons are induced in the free ligand by the exciting radiation to transfer from the lone pairs on donor atoms such as N-donors to the π-system of the fluorophores and in so doing quench their fluorescence. Involvement of these same lone pairs in forming bonds to metal ions lessens the PET quenching effect, leading to the CHEF effect, where metal ions can be sensed by the increased fluorescence intensity.[24] This can be diagrammatically illustrated in the following graphic:

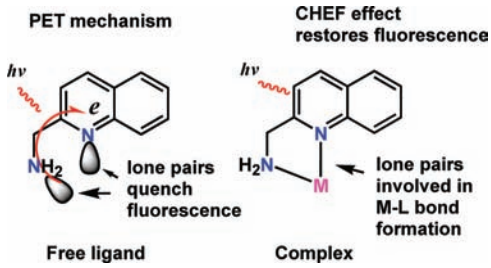

The earliest sensors for Zn(II) in biological systems, such as TSQ[1] and Zinquin[2] (see Figure 1 for key to ligand abbreviations), were based on quinolines as the fluorophores. A question that arises with these CHEF sensors for Zn(II) and Cd(II) is why some ligands show a stronger CHEF effect with Zn(II), and others with Cd(II), which can be important in selective sensing of one metal ion in the presence of the other. One detects a possible trend wherein ligand architecture that leads to elongated Zn−N bonds for the small Zn(II) ion may cause the fluorescence intensity of the Zn(II) complex to decrease relative to that for Cd(II). In the absence of such steric features, Zn(II) appears to produce a stronger CHEF effect than does Cd(II). However, the larger Cd(II) (ionic radius:[25] $r^+ = 0.96$ Å) is generally less sensitive to such steric crowding effects, which elongate Zn−N bonds, and at least partially quench fluorescence in complexes of the small Zn(II) ion ($r^+ = 0.74$ Å). It appears that a PET effect may operate from lone pairs that are only weakly involved in Zn−L bond formation and so lessen the CHEF effect, leading to stronger fluorescence with the Cd(II) complex.

In the TQEN type of ligand of Mikata et al.,[14,15] the four quinolyl groups lead to an approximately equal (TQEN) or stronger (TMQEN) CHEF effect for Cd(II) than for Zn(II). Crystal structures[14,15] reveal that two of the Zn−N bonds in the TQEN complex are very long at 2.37 and 2.40 Å, while the remaining four are close to normal, averaging 2.15 Å. The long Zn−N bonds are probably best regarded as very weak contacts at best, and the lone pairs on these nitrogen-donors (N-donors) are still able to quench fluorescence of the TQEN and TMQEN complexes to some extent by a PET mechanism. An extreme example of this may be the ligands L1 and L2, which fail to produce a CHEF effect with Zn(II) at all.[17,18] A crystal structure of the Zn(II)/L2 complex reveals very long Zn−N bonds of 2.46 Å to the two saturated N-donors of the macrocyclic ring adjacent to the phenanthroline moiety, and it has been suggested[17,18] that it is these long bonds that lead to quenching of any potential CHEF effect. Similarly, in the Zn(II) and Cd(II) complexes of the highly preorganized ligand DPP,[23] it was found that the ligand architecture favored coordination with larger metal ions with an ionic radius of about 1.0 Å and that the small Zn(II) ion should not be able to coordinate simultaneously with all four donor atoms of the ligand, leaving one lone pair free to quench the fluorescence of the ligand in its Zn(II) complex. The large Cd(II) ion can[23] coordinate simultaneously with all four donor atoms, leading to a much stronger CHEF effect than observed for Zn(II) with DPP.

In the Me_2−ZP1 sensor (Figure 1) of Goldsmith and Lippard,[12] *o*-methyl groups on the pyridines were intended to weaken the Zn(II) complex for detection of free Zn(II) concentrations in living cells. With a log K_1 value that was too high for the sensor, the Zn(II) in the cell is completely sequestered, and so, its participation in cellular function cannot be tracked.[12] The strategy of adding *o*-methyl groups to pyridyl groups is based on the well-known phenomenon

(1) Frederickson, C. J.; Kasarkis, E. J.; Ringo, D.; Frederickson, R. E. *J. Neurosci. Methods* **1987**, *20*, 91.
(2) Zalewski, P. D.; Forbes, I. J.; Betts, W. H. *Biochem. J.* **1993**, *296*, 403.
(3) Mahadevan, I. B.; Kimber, M. C.; Lincoln, S. F.; Tiekink, E. R. T.; Ward, A. D.; Betts, W. H.; Forbes, I. J.; Zalewski, P. D. *Aust. J. Chem.* **1996**, *49*, 561.
(4) Budde, T.; Minta, A.; White, J. A.; Kay, A. R. *Neuroscience* **1997**, *79*, 347.
(5) Kimura, E.; Aoki, S. *BioMetals* **2001**, *14*, 191.
(6) Harano, T.; Kikuchi, K.; Urano, Y.; Nagano, T. *J. Am. Chem. Soc.* **2002**, *124*, 6555.
(7) Burdette, S. C.; Lippard, S. J. *Coord. Chem. Rev.* **2001**, *216*, 333.
(8) Burdette, S. C.; Lippard, S. J. *Proc. Natl. Acad. Sci. U.S.A.* **2003**, *100*, 3605.
(9) Shultz, M. D.; Pearce, D. A.; Imperiali, B. *J. Am. Chem. Soc.* **2003**, *125*, 10591.
(10) Walkup, G. K.; Burdette, S. C.; Lippard, S. J.; Tsien, R. Y. *J. Am. Chem. Soc.* **2000**, *122*, 5644.
(11) Burdette, S. C.; Walkup, G. K.; Spingler, B.; Tsien, R. Y.; Lippard, S. J. *J. Am. Chem. Soc.* **2001**, *123*, 7831.
(12) Goldsmith, C. R.; Lippard, S. J. *Inorg. Chem.* **2006**, *45*, 555.
(13) Snitsarev, V.; Budde, T.; Stricker, T. P.; Cox, J. M.; Krupa, D. J.; Geng, L.; Kay, A. R. *Biophys. J.* **2001**, *80*, 1538.
(14) Mikata, Y.; Wakamatsu, M.; Kawamura, A.; Yamanaka, N.; Yano, S.; Odani, A.; Morihiro, K.; Tamotsu, S. *Inorg. Chem.* **2006**, *45*, 9262.
(15) Mikata, Y.; Wakamatsu, M.; Yano, S. *Dalton Trans.* **2005**, (3), 545–550.
(16) Gan, W.; Jones, S. B.; Reibenspies, J. H.; Hancock, R. D. *Inorg. Chim. Acta* **2005**, *358*, 3958–3966.
(17) Bazzicalupi, C.; Bencini, A.; Bianchi, A.; Giorgi, C.; Fusi, V.; Valtancoli, B.; Bernado, M. A.; Pina, F. *Inorg. Chem.* **1999**, *38*, 3806.
(18) Bazzicalupi, C.; Bencini, A.; Berni, E.; Bianchi, A.; Fornasari, P.; Giorgi, C.; Valtancoli, B. *Eur. J. Inorg. Chem.* **2003**, 1974.
(19) Miu, A. C.; Benga, O.; Adlard, P. A.; Bush, A. I. *J. Alzheimer's Disease* **2006**, *10*, 145–163.
(20) Peng, X.; Du, J.; Fan, J.; Wang, J.; Wu, Y.; Zhao, J.; Sun, S.; Xu, T. *J. Am. Chem. Soc.* **2007**, *129*, 1500.
(21) Bronson, R. T.; Michaelis, D. J.; Lamb, R. D.; Husseini, G. A.; Farnsworth, P. B.; Linford, M. R.; Izatt, R. M.; Bradshaw, J. S.; Savage, P. B. *Org. Lett.* **2005**, *7*, 1105.
(22) Charles, S.; Yunus, S.; Dubois, F.; Vander Donckt, E. *Anal. Chim. Acta* **2001**, *440*, 37.
(23) Cockrell, G. M.; Zhang, G.; VanDerveer, D. G.; Thummel, R. P.; Hancock, R. D. *J. Am. Chem. Soc.* **2008**, *130*, 1420.
(24) de Silva, A. P.; Gunaratne, H. Q. N.; Gunnlaugsson, T.; Huxley, A. J. M.; McCoy, C. P.; Rademacher, J. T.; Rice, T. E. *Chem. Rev.* **1997**, *97*, 1515.
(25) Shannon, R. D. *Acta Crystallogr., Sect. A* **1976**, *A32*, 751.

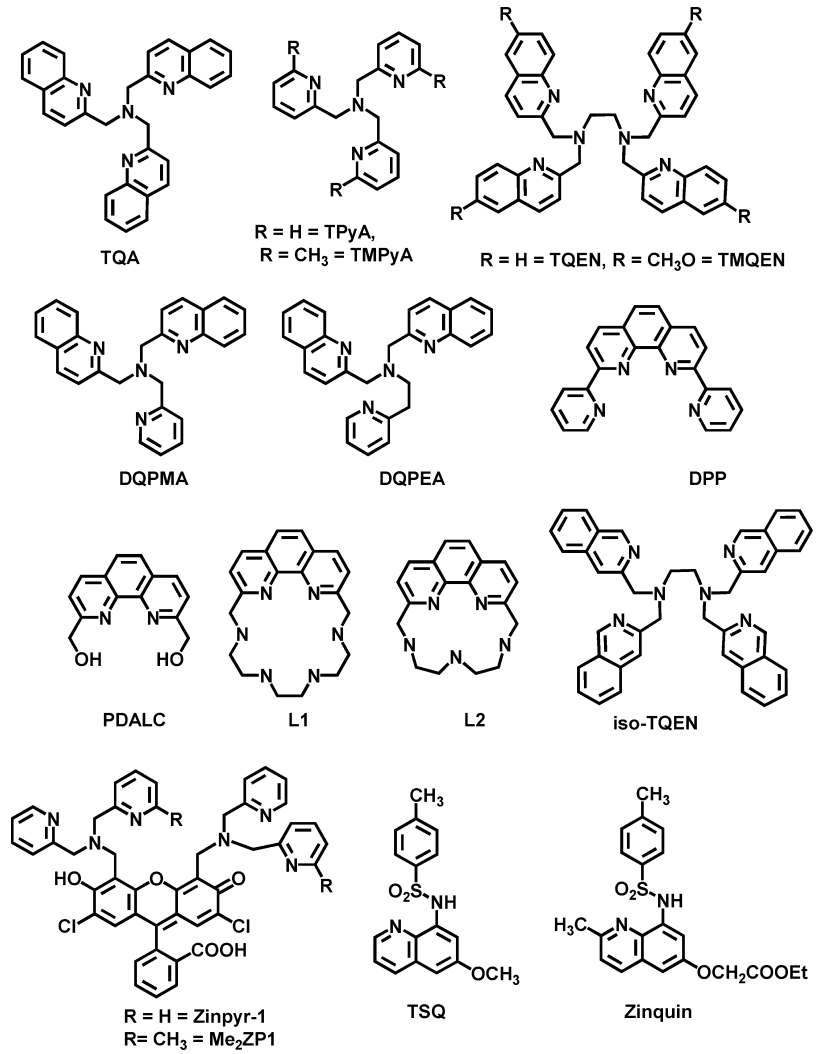

Figure 1. Ligands discussed in this Article.

that such groups are sterically crowding and lead to lower log K_1 values.[26] This is illustrated by the log K_1 values[26,27] for Zn(II) and Cd(II) with TPyA and TMPyA. For the small Zn(II) ion, log K_1 decreases[27] by 5.3 log units in passing from the TPyA complex (log K_1 = 10.88) to the TMPyA complex (log K_1 = 5.53), due to the steric crowding of the *o*-methyls of TMPyA. For the larger Cd(II), steric crowding is less serious, with a smaller drop of 3.0 log units in log K_1 in passing from the TPyA (log K_1 = 9.7) to the TMPyA complex (log K_1 = 6.72). For the very large Pb(II) ion (r^+ = 1.19 Å) the drop in log K_1 in passing from the TPyA to the TMPyA complex is only 1.7 log units. The structures[28] of TMPyA complexes generally show elongated M−N bonds to the pyridyls with their sterically hindering *o*-methyl groups. Thus, for example, in a Ni(II) complex[29] of TMPyA, the Ni−N bond to the central saturated nitrogen of the TMPyA is normal at 2.06 Å, but the Ni−N bonds to the sterically hindered pyridyl groups are very long and average 2.19 Å. Accompanying the steric crowding produced by the *o*-methyl groups in the Me_2−ZP1 ligand, Goldsmith and Lippard[12] found that the CHEF effect with Cd(II) was similar to that for Zn(II), instead of being weaker as is normally found.

In contrast to TQEN and TMQEN, the ligands DQPMA and DQPEA produce[16] a CHEF effect for Zn(II) that is considerably higher than that for the Cd(II) complexes, in line with the structure of the Zn(II)/DQPEA complex that shows[16] all of the Zn−N bonds to be of normal length. The design approach in DQPEA was[16] that the formation of a six-membered chelate ring should increase selectivity for the small Zn(II) over the large Cd(II) ion, in line with suggested ligand design rules.[30] The presence of the six-membered chelate ring also increased the CHEF effect for Zn(II) in DQPEA relative to that in Cd(II) by a factor of 3, as compared to the DQPMA complexes. One is tempted to suggest[16] that the worsened overlap in the Cd−N bond in the sterically strained six-membered chelate ring in the DQPEA complex may contribute to an enhanced PET effect and hence a decreased CHEF effect.

(26) Martell, A. E.; Smith, R. M. *Critical Stability Constant Database, 46*; National Institute of Science and Technology (NIST): Gaithersburg, MD, 2003.
(27) Anderegg, G.; Hubmann, E.; Posser, N. G.; Wenk, F. *Helv. Chim. Acta* **1977**, *60*, 123.
(28) Allen, F. H. *Acta Crystallogr., Sect. B: Struct. Sci.* **2002**, *B58*, 380.
(29) Shiren, K.; Fujinami, S.; Suzuki, M.; Uehara, A. *Inorg. Chem.* **2002**, *41*, 1598.
(30) Hancock, R. D.; Martell, A. E. *Chem. Rev.* **1989**, *89*, 1875.

The ligand TQA is an analogue of TQEN, but with its smaller number of bulky quinolyl groups, it should be less sterically crowding. One thus predicts, on the basis of the arguments presented above, that TQA being less sterically crowded should show a considerably stronger CHEF effect with Zn(II) than with Cd(II). TQA has been investigated[31,32] as a reversible Cu- or Fe-based O_2 binder. The interest in TQA in the latter work[31,32] was that the bulky quinolyl groups might sterically hinder irreversible binding of the O_2. The interest here in TQA is that the bulky quinolyl groups, like methyl groups on pyridines, should also sterically hinder coordination of metal ions. The TQA should thus have a potential for detecting metal ions by an enhanced CHEF effect due to the extensive conjugated aromatic systems of TQA and possible interesting metal ion complex stabilities and selectivities produced by the bulky quinolyl groups.

The synthesis and structures of the Zn(II), Pb(II), and Ag(I) complexes of TQA, as well as of the free TQA ligand, are reported here along with a fluorometric study of the CHEF effect in these complexes in aqueous solution and determination of the formation constants (log K_1) of TQA with a selection of metal ions by UV−visible spectroscopy.

Experimental Section

Materials. Tris(2-quinolylmethyl)amine (TQA) was synthesized by a literature method.[31] The metal perchlorates used were obtained in 99% or better purity from VWR or Aldrich and used as received. All solutions were made up in deionized water (Milli-Q, Waters Corp.) of >18 MΩ·cm^{-1} resistivity.

Synthesis of Metal Complexes. The general method for the synthesis of TQA complexes was to dissolve about 0.12 mmol of TQA with 0.12 mmol of the metal perchlorate (Zn, Ag) or nitrate (Pb) in 20 mL of 95% ethanol in a 50 mL beaker. The beaker was covered with parafilm with several small holes in it to allow for slow evaporation of the solvent. After approximately half of the solvent had evaporated after a few weeks, crystals of the metal/TQA complexes were deposited in the beaker, filtered off, and air-dried.

Synthesis of [Zn(TQA)(H_2O)](ClO_4)$_2$·1.5 H_2O (1). Synthesis as above. Colorless crystals, elemental analysis: Calcd. for $C_{30}H_{27}Cl_2N_4O_{9.5}Zn$: C, 49.23; H, 3.72; N, 7.66%. Found: C, 49.32; H, 3.52; N, 7.45%.

Synthesis of [Pb(TQA)(NO_3)$_2$]·C_2H_5OH (2). Synthesis as above. Colorless crystals, elemental analysis: Calcd. for $C_{32}H_{30}N_6O_7Pb$: C, 47.00; H, 3.70; N, 10.28%. Found: C, 46.72; H, 3.72; N, 10.54%.

Synthesis of [Ag(TQA)(ClO_4)] (3). Synthesis as above. Colorless crystals, elemental analysis: Calcd. for $C_{30}H_{24}ClN_4O_4Ag$: C, 55.62, H, 3.73; N, 8.65%. Found: C, 55.72; H, 3.53; N, 8.47%.

Structural Studies. A Bruker SMART 1K diffractometer using the omega scan mode was employed for crystal screening, unit cell determination, and data collection at 110(2) K. The structures were solved by direct methods and refined to convergence.[33] Absorption corrections were made using the SADABS program.[34] All hydrogens were located in difference Fourier maps (including those at ideal positions). Some details of the structure determinations are given in Table 1, and crystal coordinates and details of the structure determinations of **1**−**4** have been deposited with the Cambridge Structural Database (CSD).[28] A selection of bond lengths and angles for **1**, **2**, and **3** are given in Tables 2−4, and the structures of **1**−**4** are shown in Figures 2−5.

Table 1. Details of the Structure Determination of **1** ([Zn(TQA)(H_2O)](ClO_4)$_2$·1.5 H_2O), **2** ([Pb(TQA)(NO_3)$_2$]·C_2H_5OH), **3** ([Ag(TQA)(ClO_4)]), and **4** (TQA)·C_2H_5OH

	1	**2**
empirical formula	$C_{30}H_{27}Cl_2N_4O_{9.5}Zn$	$C_{32}H_{30}N_6O_7Pb$
fw	731.83	817.81
T (K)	110(2)	110(2)
cryst syst	triclinic	monoclinic
space group	$P\bar{1}$	*P21/n*
a (Å)	9.2390(11)	11.5129(14)
b (Å)	11.1243(16)	15.9845(19)
c (Å)	16.378(2)	17.495(2)
α (deg)	94.476(7)	90.00
β (deg)	96.280(7)	109.1870(10)
γ (deg)	113.491(6)	90.00
V (Å^3)	1520.8(3)	3040.7(6)
Z	2	4
μ (mm^{-1})	3.296	5.608
reflections collected	4487	6965
independent reflections	3892 (R(int) = 0.0383)	5207 (R(int) = 0.0327)
final R indices ($I > 2\sigma I$)	R1 = 0.0434	R1 = 0.0348
	wR2 = 0.1068	wR2 = 0.0826
R indices (all data)	R1 = 0.0500	R1 = 0.0551
	wR2 = 0.1115	wR2 = 0.0942
	3	**4**
empirical formula	$C_{30}H_{24}ClN_4O_4Ag$	$C_{30}H_{24}N_4$
fw	647.85	542.76
T (K)	110(2)	110(2)
cryst syst	monclinic	triclinic
space group	*C2/c*	$P\bar{1}$
a (Å)	24.540(7)	7.0897(5)
b (Å)	17.659(5)	9.1674(7)
c (Å)	14.703(4)	16.0672(11)
α (deg)	90.00	105.0240(10)
β (deg)	124.449(4)	93.9910(10)
γ (deg)	90.00	107.1270(10)
V (Å^3)	5254(2)	951.73(12)
Z	8	2
μ (mm^{-1})	0.915	1.894
reflections collected	6438	10258
independent reflections	5033 (R(int) = 0.0450)	098 (R(int) 0.0206)
final R indices ($I > 2\sigma I$)	R1 = 0.0404	R1 = 0.0330
	wR2 = 0.0935	wR2 = 0.0798
R indices (all data)	R1 = 0.0581	R1 = 0.0355
	wR2 = 0.1031	wR2 = 0.0822

Fluorescence Measurements. Excitation−emission matrix (EEM) fluorescence properties were determined on a Jobin Yvon SPEX Fluoromax-3 scanning fluorometer equipped with a 150 W Xe arc lamp and a R928P detector. The instrument was configured to collect the signal in ratio mode with dark offset using 5 nm bandpasses on both the excitation and emission monochromators. The EEMs were created by concatenating emission spectra measured every 5 nm from 250 to 500 nm at 51 separate excitation wavelengths. Scans were corrected for instrument configuration using factory supplied correction factors. Post processing of scans was performed using the FLToolbox program.[35]The software eliminates Rayleigh and Raman scattering peaks by excising

(31) Wei, N.; Murthy, N. N.; Chen, Q.; Zubieta, J.; Karlin, K. D. *Inorg. Chem.* **1994**, *33*, 1953.
(32) Wei, N.; Murthy, N. N.; Karlin, K. D. *Inorg. Chem.* **1994**, *33*, 6093.
(33) Gabe, E. J.; Le Page, Y.; Charland, J.-P.; Lee, F. L.; White, P. S. *J. Appl. Crystallogr.* **1989**, *22*, 384.
(34) Gorbitz, C. H. *Acta Crystallogr.* **1999**, *B55*, 1090.
(35) Sheldon, W. *MATLAB*, Release 11; University of Georgia: Athens, GA, 1999.
(36) Farrugia, L. J. *J. Appl. Crystallogr.* **1997**, *30*, 565.

Table 2. Selection of Bond Angles and Lengths for **1**, $[Zn(TQA)(H_2O)](ClO_4)_2 \cdot 1.5\ H_2O$

bond length (Å)					
Zn(1)−O(1W)	2.000(2)	Zn(1)−N(3)	2.082(2)	Zn(1)−N(1)	2.132(3)
Zn(1)−N(2)	2.153(4)	Zn(1)−N(4)	2.162(4)	Zn(1)−O(3)	2.71
bond angle (deg)					
O(1W)−Zn(1)−N(3)	123.69(10)		O(1W)−Zn(1)−N(1)	150.49(11)	
N(3)−Zn(1)−N(1)	85.58(11)		O(1W)−Zn(1)−N(2)	103.12(11)	
N(3)−Zn(1)−N(2)	86.31(11)		N(1)−Zn(1)−N(2)	80.50(15)	
O(1W)−Zn(1)−N(4)	93.41(11)		N(3)−Zn(1)−N(4)	98.00(10)	
N(1)−Zn(1)−N(4)	77.19(15)		N(2)−Zn(1)−N(4)	156.85(13)	

Table 3. Selection of Bond Angles and Lengths for **2**, $[Pb(TQA)(NO_3)_2] \cdot C_2H_5OH$

bond length (Å)					
Pb(1)−O(1)	2.467(3)	Pb(1)−N(4)	2.549(3)	Pb(1)−N(3)	2.622(3)
Pb(1)−N(1)	2.642(3)	Pb(1)−N(2)	2.680(3)	Pb(1)−O(6)	2.882(3)
Pb(1)−O(3)	2.914(3)	Pb(1)−O(5)	3.047(3)		
bond angle (deg)					
O(1)−Pb(1)−N(4)	74.10(11)		O(1)−Pb(1)−N(3)	86.72(11)	
N(4)−Pb(1)−N(3)	69.27(10)		O(1)−Pb(1)−N(1)	76.76(11)	
N(4)−Pb(1)−N(1)	63.54(10)		N(3)−Pb(1)−N(1)	132.59(11)	
O(1)−Pb(1)−N(2)	138.87(10)		N(4)−Pb(1)−N(2)	66.23(11)	
N(3)−Pb(1)−N(2)	69.84(11)		N(1)−Pb(1)−N(2)	94.41(10)	
N(5)−O(1)−Pb(1)	107.8(2)				

Table 4. Selection of Bond Angles and Lengths for **3**, $[Ag(TQA)(ClO_4)]$

bond length (Å)					
Ag(1)−N(3)	2.396(3)	Ag(1)−N(4)	2.416(3)	Ag(1)−N(2)	2.426(3)
Ag(1)−N(1)	2.485(3)	Ag(1)−O(1)	2.572(2)		
bond angle (deg)					
N(3)−Ag(1)−N(4)	112.04(8)		N(3)−Ag(1)−N(2)	110.84(9)	
N(4)−Ag(1)−N(2)	103.95(9)		N(3)−Ag(1)−N(1)	70.87(9)	
N(4)−Ag(1)−N(1)	69.86(9)		N(2)−Ag(1)−N(1)	69.33(8)	
N(3)−Ag(1)−O(1)	116.03(9)		N(4)−Ag(1)−O(1)	104.08(8)	
N(2)−Ag(1)−O(1)	109.03(8)		N(1)−Ag(1)−O(1)	172.59(8)	

portions (±10−15 nm FW) of each scan centered on the respective scatter peak. Following removal of scatter peaks, data were normalized to a daily determined water Raman intensity (275ex/303em, 5 nm bandpasses). Replicate scans were generally within 5% agreement in terms of intensity and within bandpass resolution in terms of peak location. The fluorescence spectra of 2×10^{-5} M TQA were recorded in 50% methanol/water.

Formation Constant Studies. These were determined by UV−visible spectroscopy following procedures similar to those of Xia et al.[37] for studying 1,10-phen complexes. UV−visible spectra were recorded using a Varian 300 Cary 1E UV−visible spectrophotometer controlled by Cary Win UV scan application version 02.00(5) software. A VWR sympHony SR60IC pH meter with a VWR sympHony gel epoxy semimicro combination pH electrode was used for all pH readings, which were made in the external titration cell, with N_2 bubbled through the cell to exclude CO_2. The pH meter was calibrated prior to every titration, using standard acid−base titration procedures. The cell containing 50 mL of ligand/metal solution was placed in a bath thermostatted to 25.0 ± 0.1 °C, and a peristaltic pump was used to circulate the solution through a 1 cm quartz flow cell situated in the spectrophotometer. The pH was altered in the range 2−10 by additions to the external titration cell of small amounts of $HClO_4$ or NaOH as required, using a micropipette. After each adjustment of pH, the system was allowed to mix by operation of the peristaltic pump for 15 min prior to recording the spectrum, and the cell was also agitated with a magnetic stirrer bar to ensure complete mixing.

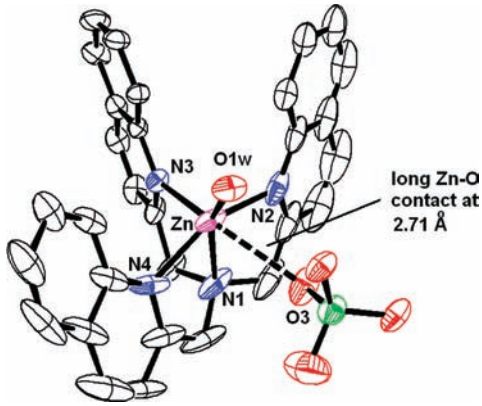

Figure 2. ORTEP[36] drawing of the complex cation $[Zn(TQA)(H_2O)]^{2+}$ in **1** showing the numbering scheme for donor atoms around the Zn(II) ion. H atoms omitted for clarity. Thermal ellipsoids drawn at the 50% probability level.

The ligand TQA has low water solubility ($\sim 10^{-5}$ M) but can be studied spectrophotometrically at such concentrations because of the intense bands in the UV in the 200−350 nm range. An unusual problem that was encountered was that the first two protonations (pK_1 and pK_2) of the ligand produce only a small change in the UV spectrum (Figure 6(a) and (b). By analogy with ligands such as TPA, studied by Anderegg et al.,[27] one would expect a pK_1 for TQA of 6.1, a pK_2 of 4.3, and a pK_3 of 2.5. Large changes in the UV spectrum of TQA occur only for an equilibrium that occurs with a pK of 2.49, which would correspond to pK_3 for TPA. An equilibrium at higher pH produced very small changes in the spectra of the TQA solutions and yielded a pK of 3.0 ± 0.1, which would correspond to pK_2 for TPA. The changes in the spectra in the vicinity of pH 6, which is where one would expect pK_1 for TQA to occur, were also small and yielded a value of 6.3 ± 0.1 for the first protonation constant. The pK values reported (Table 5) here were fitted to the variation of absorbance (Figure 6(a)) at 10

(37) Xia, Y. X.; Chen, J. F.; Choppin, G. R. *Talanta* **1996**, *43*, 2073.

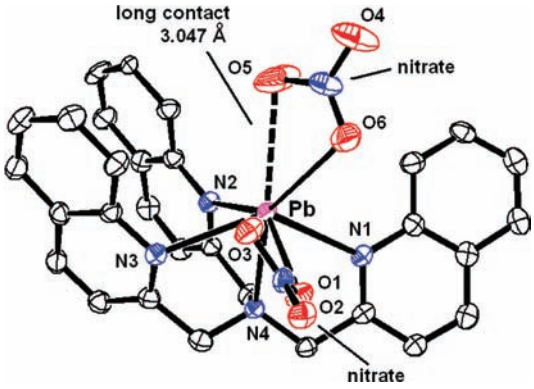

Figure 3. ORTEP[36] drawing of the complex $[Pb(TQA)(NO_3)_2]$ in **2**. H atoms omitted for clarity. Thermal ellipsoids drawn at the 50% probability level.

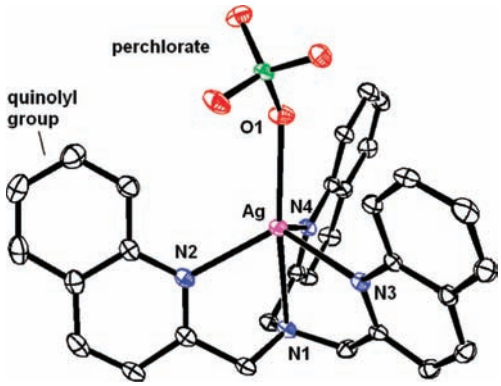

Figure 4. ORTEP[36] drawing of the complex $[Ag(TQA)(ClO_4)]$ in **3** showing the numbering scheme for donor atoms around the Ag(I) ion. H atoms omitted for clarity. Thermal ellipsoids drawn at the 50% probability level.

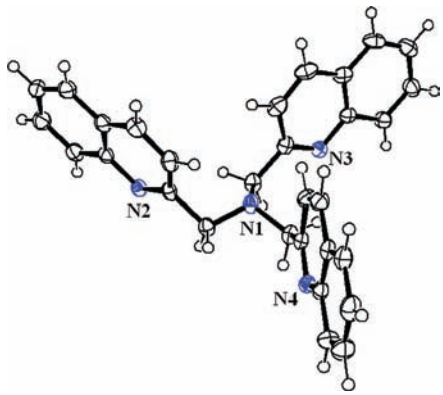

Figure 5. ORTEP[36] drawing of **4**, the free ligand TQA. Thermal ellipsoids drawn at the 50% probability level.

wavelengths for a 2×10^{-5} *M* TQA solution (Figure 6(b)) using the SOLVER module of EXCEL.[38] The standard deviations on log *K* values reported here were determined using the SOLVSTAT macro provided with ref 38. The formation constants for Zn(II), Cd(II), and Pb(II) reported in Table 5 were obtained from the variation of absorbance for 1:1 mixtures of 2×10^{-5} *M* M^{2+} and TQA.

Results and Discussion

Structural Studies. The structure of **1**, the Zn(II) complex cation with TQA, is seen in Figure 2. The Zn is 5-coordinate

(38) Billo, E. J. *EXCEL for Chemists*; Wiley-VCH: New York, 2001.

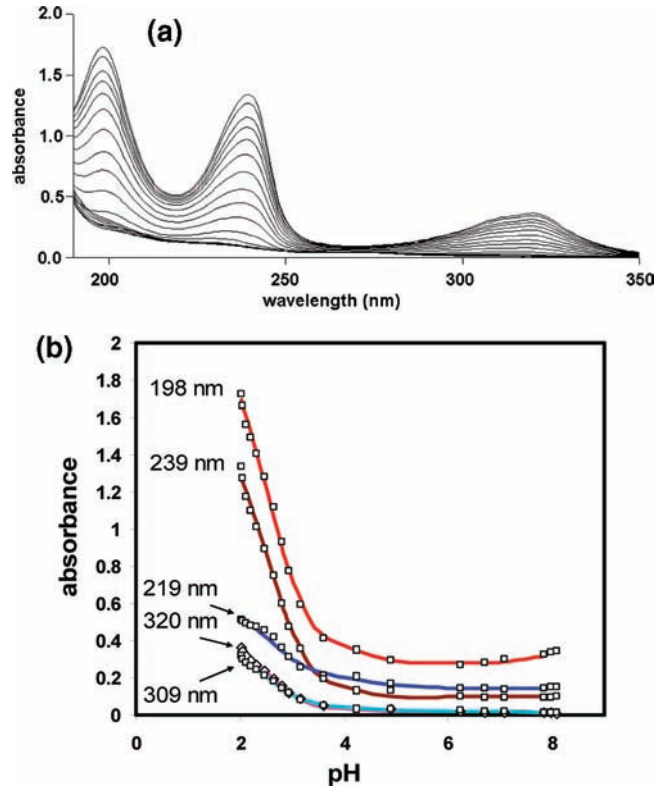

Figure 6. (a) Spectra of 2×10^{-5} *M* TQA in 0.1 *M* $NaClO_4$ at 25.0 °C in the pH range from 2.02 (uppermost spectrum) to 8.09 (lowest spectrum). (b) Fitting of theoretical absorption vs pH curves (solid lines) to the experimental points at five wavelengths for 2×10^{-5} *M* TQA in 0.1 *M* $NaClO_4$ at 25 °C. Theoretical curves were fitted using EXCEL[21] as described in the text. To avoid cluttering only 5 of the 10 wavelengths used for the fitting are shown.

Table 5. Formation Constants for TQA (L) Determined Here[a]

equilibrium	log *K*	reference
$H^+ + OH^- \leftrightarrows H_2O$	13.78	18
$L + H^+ \leftrightarrows LH^+$	6.3(1)	this work
$LH^+ + H^+ \leftrightarrows LH_2^{2+}$	3.0(1)	this work
$LH_2^{2+} + H^+ \leftrightarrows LH_3^{3+}$	2.49(2)	this work
$L + Zn^{2+} \leftrightarrows ZnL^{2+}$	8.7(2)	this work
$L + Cd^{2+} \leftrightarrows CdL^{2+}$	8.7(2)	this work
$L + Pb^{2+} \leftrightarrows PbL^{2+}$	8.6(2)	this work

[a] For key to ligand abbreviations, see Figure 1.

with four N-donors from TQA and a water molecule coordinated to the Zn. There is a long contact with an oxygen (O3) from a perchlorate, at 2.71 Å, but this is probably too long to be regarded as a bond. The important factor here is that the Zn−N bonds to the three quinolyl nitrogens, which range from 2.083 to 2.153 Å, as well as the Zn−N bond to the saturated nitrogen of TQA (2.132 Å) show no signs of bond-length distortion. The mean length for Zn−N bonds to quinolines and quinoline-like ligands (1,10-phenanthroline, 8-hydroxyquinoline, etc.) found in the CSD[28] (383 hits) is 2.136 ± 0.062 Å. The Zn−N bonds in the Zn/TQA complex are thus well within the range for normal Zn−N bonds with quinoline-like ligands, so that, unlike the Zn(II)/TQEN complex, where Zn−N bonds involving quinolines are[14] as long as 2.40 Å, one can conclude that there is little sign of distortion of the Zn−N bonds in TQA. In terms of the idea put forward here, the long Zn−N bonds to quinolines in the Zn/TQEN complex may contribute to weakening the fluo-

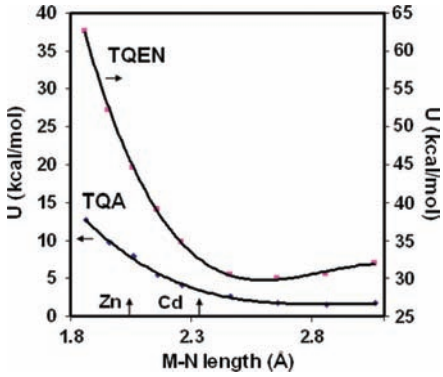

Figure 7. Strain energy (U) for $[M(TQA)(H_2O)]^{n+}$ and $[M(TQEN)]^{n+}$ complexes as a function of M−N bond length. Note that, in order to facilitate comparison, the curve for the TQEN complexes has been lowered and refers to the right-hand scale for U, while that for the TQA complexes refers to the left-hand scale.

rescence intensity, whereas with the Zn/TQA complex the structure shows no sign of such distortions, in accord with the very high fluorescence intensity of the Zn(II)/TQA complex relative to the Cd(II)/TQA complex.

One can use molecular mechanics[39,40] (MM) to scan the strain energy of a complex to see what happens to the strain energy as a function of metal ion size. The calculations were performed with HyperChem,[41] which contains the MM+ force field, which is essentially the MM2 force field[42] with additional parameters to allow for modeling of complexes of metal ions. The structures used for the MM calculations were the reported[15] structure of $[Zn(TQEN)]^{2+}$ and the structure of $[Zn(TQA)(H_2O)]^{2+}$ reported here. The calculations were carried out with all default parameters relating to the Zn(II) ion, except that the M−N force constant was kept constant at 0.5 mdyne·Å^{-1}, as a representative value for a range of metal ions. The equilibrium M−N bond lengths were varied in 0.1 or 0.2 Å increments from 1.9 to 3.1 Å, calculating U for the complexes at each point. Plots of U versus the equilibrium M−N bond length for $[M(TQEN)]^{n+}$ and $[M(TQA)(H_2O)]^{n+}$ complexes are seen in Figure 7. The strain energies of the $[M(TQEN)]^{n+}$ complexes are considerably higher than those for the $[M(TQA)(H_2O)]^{n+}$ complexes, so in order to facilitate comparison, the curve for the $[M(TQEN)]^{n+}$ complexes has been lowered by 25 kcal·mol^{-1}. One cannot compare strain energies of two different complexes directly, but what one can see is that the strain energy of the $[M(TQEN)]^{n+}$ complexes rises very much more rapidly than that for the $[M(TQA)(H_2O)]^{n+}$ complexes at M−N bond lengths below about 2.5 Å. The ideal M−N bond lengths for Zn(II) (2.136 Å) and Cd(II) (2.362 ± 0.045 Å, 216 hits in the CSD[28]) are indicated on Figure 7. One sees that Cd(II) is large enough that it is close to the minimum value of U for both the $[M(TQEN)]^{n+}$ and $[M(TQA)(H_2O)]^{n+}$, and no Cd−N bond length distortion is expected. For Zn(II) in the $[M(TQA)(H_2O)]^{n+}$ complex, the rise in strain energy is still quite small, but for the $[M(TQEN)]^{n+}$ complex, a considerable rise is expected, with accompanying Zn−N bond length distortion. Interestingly, at an appropriate Zn−N ideal bond length of 2.15 Å, the MM calculations predict a structure for $[Zn(TQEN)]^{n+}$ that has the appropriate Zn−N bond lengths stretched out to roughly 2.4 Å, as observed in the experimental structure.[15] The calculations in Figure 7 support the suggestion that the TQEN complex of Zn(II) is sterically very crowded and so has Zn−N bond length distortion, whereas the TQA complex is not very sterically crowded and so does not have Zn−N bond length distortion.

Table 6. Formation Constants (Log K_1) for TQA Compared to Those for TPyA and TMPyA[a]

ligand	ionic radius (Å)	log K_1(TQA)	log K_1(TPyA)	log K_1(TMPyA)
Zn(II)	0.74	8.7	10.88	5.53
Cd(II)	0.96	8.6	9.7	6.72
Pb(II)	1.19	8.7	8.5	6.73

[a] For key to ligand abbreviations, see Figure 1. Log K_1 values for TQA (this work) and for TPyA and TMPya (refs 7 and 27). Ionic radii for 6-coordinate metal ions from ref 25.

The complex $[Pb(TQA)(NO_3)_2]$ in **2** is shown in Figure 3 and is included here as an example of a large metal coordinated to TQA. A reviewer has quite correctly commented that the Cd(II) structure of TQA would be the best indication of this, but unfortunately, we were not able to obtain crystals of the Cd(II) complex. The Pb is possibly 8-coordinate comprising the four N-donors of TQA and two bidentate nitrates. There is the usual problem with Pb(II) complexes in that bonds close to the probable site of the lone pair may be rather long,[43−45] so that one has some difficulty in deciding whether the longer Pb−L contacts are to be regarded as bonds. The shortest Pb−L bonds (L = ligand donor atom) are opposite the site of the lone pair,[43−45] while the Pb−L bonds become systematically longer as they are closer to the site of the lone pair. Thus, Pb−O(1) is quite short at 2.467 Å, while the three bonds that are close to the possible site of the lone pair, opposite the saturated nitrogen (N(4)) of TQA, are rather long, ranging from 2.882 to 3.047 Å. One can see in Figure 3, as is usually the case,[43−45] that bonds close to N(4) are short, with the longest Pb−O bond (Pb(1)−O(5) = 3.047 Å) being most nearly opposite the saturated N-donor, with N(4)−Pb(1)−O(5) = 167.5°.

The structure of **3**, which is the complex $[Ag(TQA)ClO_4]$, is seen in Figure 4. The interest in this structure is that the Ag(I) (r^+ = 1.0 Å) is about the same size as Cd(II) (r^+ = 0.96 Å) and so should indicate how well Cd(II) should coordinate with TQA. The Ag is 5-coordinate with four N-donors from the TQA ligand and an O-donor from the perchlorate. The Ag(I) in **3** shows little distortion toward linear coordination geometry, which is often observed[45] for heavy d^{10} metal ions, particularly Au(I) and Hg(II). The average Ag−N bonds to pyridyl-type groups in the CSD (161 hits) for 5-coordinate Ag(I) is 2.35 ± 0.16 Å, so that the

(39) Hancock, R. D. *Acc. Chem. Res.* **1990**, *23*, 253.
(40) Hancock, R. D. *Prog. Inorg. Chem.* **1989**, *36*, 187–291.
(41) *Hyperchem Program*, Version 7.5; Hypercube, Inc.: Waterloo, Ontario, Canada.
(42) Allinger, N. L. *J. Am. Chem. Soc.* **1977**, *98*, 8127.
(43) Shimoni-Livny, L.; Glusker, J. P.; Bock, C. W. *Inorg. Chem.* **1998**, *37*, 1853.
(44) Hancock, R. D.; Shaikjee, M. S.; Dobson, S. M.; Boeyens, J. C. A. *Inorg. Chim. Acta* **1988**, *154*, 229.
(45) Hancock, R. D.; Reibenspies, J. H.; Maumela, H. *Inorg. Chem.* **2004**, *43*, 2981.

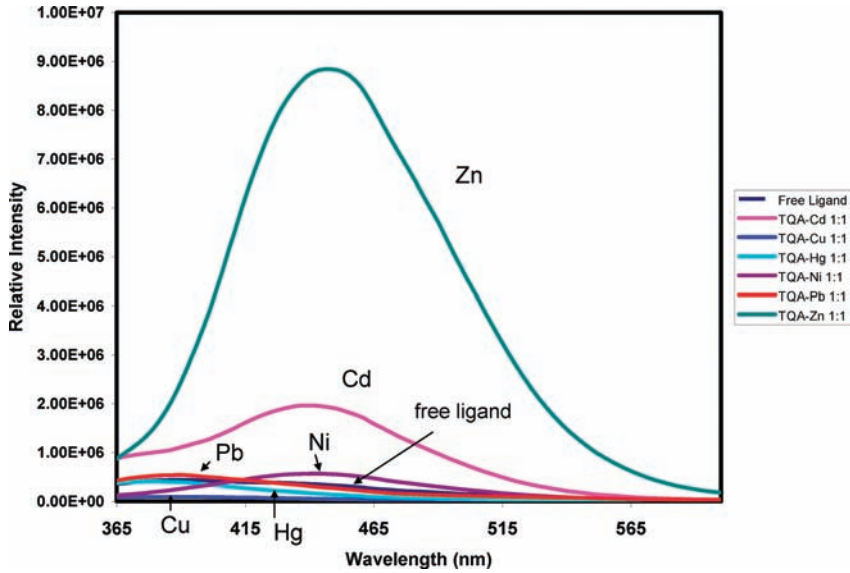

Figure 8. Fluorescence spectra of TQA (10^{-5} *M*) in 50% methanol/water at pH ~ 7.0 and some TQA complexes with metal ions (all 10^{-5} *M*). The wavelength of the exciting radiation is 317 nm. The fluorescence peak for the Zn/TQA complex is at 445 nm, while that of free TQA is at 390 nm.

Ag−N bonds in **3**, which range from 2.396 to 2.485 Å (Table 4), are slightly on the long side, which probably reflects the fact that, at an M−N length of about 2.35 Å, Figure 7 suggests that there would be a small amount of M−N bond length stretching. The Ag(I) is a good example of coordination of a large metal ion ($r^+ = 1.15$ Å) coordinating with TQA, and the structure shows that, at this metal ion radius, there would be little bond length distortion, which should also be true for the large Cd(II) ion.

Formation Constant Studies. The formation constants measured here for TQA complexes are seen in Table 5. The constants are somewhat lower than those[27] for the TPyA complexes but considerably higher than those[27] for TMPyA, as seen in Table 6. One sees that the smaller the metal ion, the greater is the drop in log K_1(TQA) compared to log K_1(TPyA). The results are in accord with the suggestion[16] that the quinaldine groups of TQA lead to greater steric crowding than is true for the picolyl groups of TPyA but much less than that induced by the *o*-methyl substituted pyridyl groups of TMPyA. A reviewer has raised the question of why the log K_1 values for TQA are almost constant for Zn(II), Cd(II), and Pb(II). One would suggest that the order of log K_1 for TPyA, which is (Table 6) Zn(II) > Cd(II) > Pb(II), represents the intrinsic low-strain order. For TMPyA, the *o*-methyl groups on the pyridines produce high levels of steric crowding, which results in a size-based reversal of order of log K_1 to Zn(II) < Cd(II) < Pb(II), which is the order of increasing ionic radius.[25] The level of steric crowding in TQA complexes is less than that in the TMPyA complexes and so appears to produce a balance in stability such that no trend in log K_1 is observed along the series.

Fluorescence Studies. Figure 8 shows the emission spectra of TQA and its complexes with a selection of metal ions at a concentration of 10^{-5} *M* at pH ~ 7 in 50% methanol/water, with excitation at 317 nm. The relative emission intensities of the free ligand and the metal ion complexes of TQA are presented as a bar chart in Figure 9. The emission spectrum of Zn(II) is much more intense than

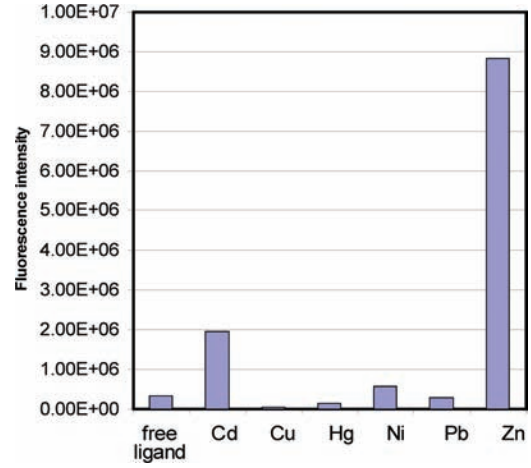

Figure 9. Fluorescence intensity at 445 nm in 50% methanol/water for the free ligand of TQA plus some of its 1:1 complexes with metal ions (all at 10^{-5} *M* and pH = 7.0), with the exciting wavelength being 317 nm.

that of Cd(II), as would be expected from the idea[17,18] that Zn−N bond length distortion leads to quenching of the CHEF effect in complexes of Zn(II) and the structure of $[Zn(TQA)H_2O]^{2+}$ reported here shows no evidence of such Zn−N bond lengthening. In contrast, the $[Zn(TQEN)]^{2+}$ complex shows[14,15] considerable Zn−N bond distortion, with a concomitant decrease in the CHEF effect of the Zn(II) complex compared to the Cd(II) complex, which is not expected to show such M−N bond length distortion.

Interestingly, as this manuscript was completed, the authors became aware of the online paper of Mikata et al.[46] who report the fluorescence properties of the isoquinoline analogue of TQEN, which is iso-TQEN in Figure 1, which is not nearly as sterically crowding as TQEN. The structure shows[46] that $[Zn(iso\text{-}TQEN)]^{2+}$ does not suffer significant Zn−N bond length stretching, and in accord with the ideas advanced here, the CHEF effect for the Zn(II)·iso-TQEN

(46) Mikata, Y.; Yamanaka, N.; Yamashita, A.; Shigenobu, Y. *Inorg. Chem.*, in press.

complex is many times larger than that for the Cd(II)/iso-TQEN complex.

One sees that, for a variety of Zn(II) and Cd(II) complexes,[14−18,23] the idea that elongation of the Zn−N bonds by steric crowding will lead to a partially restored PET effect and hence a diminished CHEF effect for the Zn(II) relative to the Cd(II) complex, which is borne out by the results reported here for the TQA complexes, where normal Zn−N bond lengths lead to a very much stronger CHEF effect than for the Cd(II) complex, as borne out in Figures 8 and 9. One problem with the thesis here of steric crowding leading to a stronger CHEF effect with Cd(II) than Zn(II) is the reported[20] strong fluorescence with Cd(II) and not Zn(II) of a sensor based on a dipicolylamine ligand attached to a fluorophore. These authors do not report a structure of the Zn(II) or Cd(II) complex with their ligand, so one cannot be sure of the coordination sphere around the Zn(II) or Cd(II). However, the Zinpyr-1 sensor (Figure 1) of Lippard et al.[10,11] also features binding of the metals to a dipicolylamine group, and here, the CHEF effect with Zn(II) is strong. A search of the CSD[28] shows that for Zn(II) coordinated to dipicolylamine or ligands with dipicolylamine fragments, the Zn−N bonds to the pyridyl groups average 2.10 ± 0.06 Å (167 hits) and those to the saturated N-donor average 2.22 ± 0.06 Å. The lengthening of the bond to the saturated N-donor is quite normal for a sp^3 hybridized N-donor as compared to the sp^2 hybridized pyridine-type N-donor. Thus, for Cd(II) complexes of dipicolylamine type ligands[28] (17 hits), the Cd−N lengths to the sp^2 hybridized pyridyl groups average 2.36 ± 0.07 Å, while those to the saturated sp^3 hybridized N-donor average 2.50 ± 0.12 Å. Clearly, some additional factor is present in the Cd(II) sensor of Peng et al.,[20] which leads to a stronger CHEF effect with Cd(II) than Zn(II), which would be of considerable interest to investigate.

Conclusions

The results presented here support the emerging idea[16−18,23] that steric effects that lead to bond length distortion can lead to diminution of the CHEF effect in complexes. This may result because with poor overlap in the Zn−N bond, the electrons on the N-donor groups are more available to participate in a PET effect and so partially quench the fluorescence of the Zn(II) complex. In the case of TQEN,[14,15] steric crowding is less severe for the larger ion and for the smaller ion leads to Zn−N bond length distortion, which allows some quenching of fluorescence by the photoinduced electron transfer (PET) mechanism. TQA is a less sterically crowding ligand than TQEN, which should lead to less distortion of the M−N bonds and hence a lessened PET quenching of fluorescence. This idea is supported by the structure of $[Zn(TQA)(H_2O)]^{2+}$, which shows no significant Zn−N bond length distortion, in contrast to[14,15] $[Zn(TQEN)]^{2+}$. This is in accord with the observation here that the CHEF effect in the Zn(II)/TQA complex is much larger than that in the Cd(II)/TQA complex, while for the TQEN complexes, the difference between the CHEF effect in the Zn(II) and Cd(II) complexes is much smaller.[14,15]

Acknowledgment. The authors thank the University of North Carolina, Wilmington, and the National Science Foundation (Grant No. CHE-0111131) for generous support for this work.

IC801403S